NASA Technical Memorandum 103157

High Temperature Fatigue Behavior of a SiC/Ti-24Al-11Nb Composite

P.A. Bartolotta and P.K. Brindley
Lewis Research Center
Cleveland, Ohio

Prepared for the
10th Symposium on Composite Materials: Testing and Design
sponsored by the American Society for Testing Materials
San Francisco, California, April 24–25, 1990

NASA

HIGH TEMPERATURE FATIGUE BEHAVIOR OF A SIC/TI-24AL-11NB COMPOSITE

P.A. Bartolotta and P.K. Brindley
National Aeronautical and Space Administration
Cleveland, OH 44135

SUMMARY

A series of tension-tension strain- and load-controlled fatigue tests were conducted on unidirectional SiC/Ti-24Al-11Nb (at %) composites at 425 and 815 °C. Several regimes of damage were identified using Talreja's (ref. 1) concept of fatigue life diagrams. Issues of test technique, test control mode, and definition of failure were also addressed.

INTRODUCTION

The intermetallic composite SiC/Ti-24Al-11Nb (at %) has generated considerable interest for aerospace applications due to its high strength to density ratio. Recent investigations have examined various aspects of this composite such as fiber-matrix chemical interactions (refs. 2 to 7), fiber-matrix bond strength (ref. 8), tensile properties (refs. 2, 3, and 9), and thermal cycling (refs. 10 and 11). However, only one study to date has examined the fatigue behavior of this composite (ref. 12). Further study of SiC/Ti-24Al-11Nb is necessary for complete understanding of fatigue behavior and damage mechanisms. The current study examined the fatigue response of unidirectional SiC/Ti-24Al-11Nb isothermally fatigued at 425 and 815 °C. The influence of test methodology (strain- versus load-control) on failure mechanisms was also a major topic of this investigation. This study is the first portion of an on-going examination of fatigue properties and damage mechanisms in SiC/Ti-24Al-11Nb.

EXPERIMENTAL PROCEDURE

The SiC/Ti-24Al-11Nb composites were fabricated by the powder cloth technique (ref. 13) followed by vacuum hot pressing (VHP). The fiber used was the 140 μm diameter, double-coated, SCS-6 SiC manufactured by Textron, Inc. The matrix material was Ti-24Al-11Nb and was obtained as prealloyed PREP powder. The composites were produced with three plies of continuous fibers oriented in the 0° direction (parallel to the loading axis during testing) with an approximate volume fraction of 27 percent. Composite plates typically measured 150 mm long x 50 mm wide x 0.7 to 0.8 mm thick. Consolidated plates were etched in nitric acid to remove the Mo cladding required during VHP. Typical fiber distribution in the fully consolidated composite is shown in figure 1(a). As shown in figure 1(b), the composite microstructure was quite complex. The matrix was comprised of equiaxed α_2 (Ti_3Al) surrounded by disordered β. A β-depleted zone was present in the matrix adjacent to the fiber-matrix reaction zone which surrounded the C-rich coating of the fiber. A more extensive analysis of this as-fabricated composite microstructure has been previously performed by scanning transmission electron microscopy (ref. 4).

Composite specimens were wire electrodischarge machined (EDM) from the plate as shown in figures 2(a) and (b). The specimen design incorporated a reduced, parallel-sided test section to facilitate close control of the temperature profile and a large fillet radius of 60 mm to minimize failures near the radius. After EDM, specimen surfaces were polished with 180 grit SiC paper to remove a 10 μm cladding reaction with the Mo release sheets used during fabrication and to remove damage due to wire EDM. Tabs, as shown in figure 2(b), were applied with epoxy. This increased the gripped-section thickness to approximately 6 mm, nearer to that of the grip opening, to help minimize possible bending stresses due to gripping. Tabs were tapered to distribute through-thickness stresses resulting from high clamping forces. The use of the above specimen and tab designs produced fracture within the gage section in 93 percent of the specimens.

The experiments were conducted under computer control on a closed-loop, servo-hydraulic system with a 222 kN maximum load capacity. A derated load capacity of 9 kN full scale was used. Water-cooled, hydraulic grips were aligned independent of the specimen to a tolerance of <3 percent bending during initial installation. The experimental equipment, data acquisition, and computer control system has been previously described (ref. 14). A standard 12.7 mm gage length extensometer was mounted on the edge of the sample in order to avoid possible bending induced by mounting the extensometer on the width of the specimen. The specimens were heated by a two-zone direct resistance furnace specifically designed for the plate specimens (ref. 15). This furnace maintained a temperature profile in the test section of ±1 percent of the nominal value. Beaded type K thermocouples were tied onto the test section. Specimens were maintained at temperature for 1 hr prior to testing to allow the equipment to stabilize. Note that 1 hr at the highest temperature of 815 °C causes negligible growth of the fiber-matrix reaction zone (ref. 3).

To address the issue of test control method, fatigue tests were conducted in both strain-control and load-control at 425 and 815 °C. Strain-controlled tests were conducted using a triangular control waveform which was limited by the required maximum strain and zero load. The strain rate was $1x10^{-3}$ sec^{-1}. Load-controlled tests also used a triangular control waveform in which load was limited by the maximum required load and zero load. The loading rate and maximum load limits were selected to parallel the strain rate and maximum loads achieved in the strain-controlled tests. For some of the higher load limits, a hybrid program was substituted for the load-controlled tests. The hybrid program was strain-controlled but had load limits at the maximum and minimum points of the cycle instead of strain limits. This was necessary because some of the large loads achieved in strain-controlled tests could not be achieved in load-control since the material response caused an instability in the control loop.

RESULTS AND DISCUSSION

Fatigue Life Relationships

Fatigue life results for the SiC/Ti-24Al-11Nb composite at 425 and 815 °C are presented in figure 3 for both strain- and load-controlled test conditions. A fatigue life diagram was created after Talreja (ref. 1) by plotting the data as maximum strain versus number of cycles to failure. Fatigue lives of the strain- and load-controlled tests were compared on a maximum strain basis since, in the absence of cracking or debonding, the strain for both the fiber and the matrix are the same during a test but the stresses in the composite constituents differ (ref. 16). The data displayed three distinct regions, identified for this work as Regions I to III. Regions I and III did not vary with test temperature while Region II was clearly temperature dependent. These three regions were similar in shape to those of the fatigue life diagram for a polymer matrix composite at 23 °C (ref. 1) as shown in figure 4. It should be noted that failure of the SiC/Ti-24Al-11Nb composite specimens in figure 3 was defined as fracture into two pieces except for the strain-controlled tests in Region II where failure was defined as the first simultaneous decrease in stress and stiffness of ≥30 MPa and 10 GPa, respectively, as will be discussed shortly.

For the SiC/Ti-24Al-11Nb composite, Region I of figure 3 was approximately bounded by the tensile ductility ranges for this composite, which were independent of test temperature at 425 and 815 °C, at values of 0.69 to 0.85 percent (ref. 9). It was previously suggested that the tensile properties of SiC/Ti-24Al-11Nb were dominated by the SiC fiber over a temperature range of 23 to 815 °C (ref. 9). This was because the composite failed at strains slightly less than or equal to the fiber strain-to-failure at all temperatures tested while the total strain-to-failure of the matrix increased from 1.6 to 20.6 percent over the temperature range. Likewise, it is reasonable to suggest that fiber strain-to-failure also largely affected the fatigue behavior of this composite at 425 and

815 °C within Region I, especially since several tests failed upon load-up. Furthermore, the probabilistic failure nature of this composite in tension was attributed to variations in fiber strength (and thus, fiber strain-to-failure), both between fiber lots and within a fiber lot (ref. 9). Fiber strength variability within a given specimen would be expected to mimic the variability within a given fiber lot. Therefore, variations in fiber strengths and thus, variations in fatigue lives, were also expected within this high strain Region I. In fact, fatigue lives for the SiC/Ti-24Al-11Nb composite ranged from 1/4 cycle to approximately 700 cycles at 815 °C and from 1/4 cycle to approximately 20 000 cycles at 425 °C in this region. This apparent dominant effect of fiber failure does not exclude other operative mechanisms.

With one exception, failure within Region I occurred by complete fracture and was defined as catastrophic or nonprogressive since the material response gave only minor indications of the impending failure. The typical maximum and minimum stress response as a function of cycles is shown in figure 5 for specimens at 425 and 815 °C. By test design, the load-controlled tests showed a constant maximum stress until failure. A typical specimen tested in strain-control at 425 °C displayed a relatively constant stress response until the last few thousand cycles before failure in which stress slowly decreased by 40 MPa. At 815 °C, typical strain-controlled specimens displayed stress decreases which totaled approximately 45 MPa in the first several cycles, as well as additional stress decreases which totaled about 55 MPa in the last several hundred cycles before failure.

Figure 6 shows maximum and minimum strain as a function of cycles for samples in Region I at 425 and 815 °C. Again, by design, strain-controlled tests exhibited a constant maximum strain throughout the tests. The increases in minimum strain for the strain-controlled tests were artifacts of the control program which did not allow the composite to go into compression and will be discussed shortly. Specimens tested in load-control exhibited ratchetting up to 0.05 percent strain at 425 °C, which was approximately 10 percent of the total strain range, and up to 0.13 percent strain at 815 °C, which was approximately 23 percent of the total strain range.

The elastic modulii (E) for both strain- and load-controlled specimens within Region I are shown in figure 7. E remained constant, within experimental error, at both 425 and 815 °C until the last cycles of life during which it appeared to decrease. This slight decrease in E was most noticeable in the strain-controlled tests. An E of 168 GPa at 425 °C was obtained in this study as compared with the E obtained in tension of 180 GPa (ref. 9). E values of 151 to 157 GPa were obtained at 815 °C and were slightly greater than the previous E values obtained in tension of 138 GPa (ref. 9). One possibility for the differences in E is variation in fiber volume for samples tested in tension and those of this study; volume fraction of fibers has been determined for each individual tensile specimen (ref. 9) but is only approximately known for the samples of this study.

Fatigue behavior within Region II of figure 3 was defined as progressive because the mechanical response of the strain-controlled tests at both 425 and 815 °C first displayed gradual decreases in the maximum stress and then abrupt, simultaneous decreases in the maximum stress (σ_{MAX}) and unloading modulus with continued cycling, as shown in figures 8 and 9. Furthermore, the specimens typically remained intact after these abrupt indications of damage. With these evidences of damage accumulation throughout the life of the composite, it became necessary to define failure for the strain-controlled tests in Region II as something other than final fracture, as has been suggested by Salkind (ref. 17). Thus, failure for the strain-controlled tests in Region II of this work was defined as the cycle at which the first abrupt sign of damage was observed (e.g., the first abrupt, simultaneous decrease in stress and modulus). In the lower strain portion of Region II, this initial degradation in strength and modulus was approximately 30 MPa and 10 GPa, respectively, and increased as the strain range was increased. However, the load-controlled specimens did not display these stress drops, as shown in figure 8, but failed catastrophical-

ly by complete fracture of the specimen. It can be seen in figure 3 that the above definition of failure in strain-control was a reasonable approach since, at a given temperature, failure in strain-control corresponded well with complete fracture in load-control. And as previously mentioned, Region II of figure 3 displayed temperature dependent fatigue behavior in which specimens tested at 425 °C had longer lives than those tested at 815 °C at the same strain amplitude.

Figures 10 to 13 show typical stress-strain responses of the SiC/Ti-24Al-11Nb composite within Region II of figure 3. Comparison of the responses from the strain- and load-controlled tests under conditions with similar initial values of strain and stress at a given temperature are presented for the 425 °C tests in figures 10 and 11 and for the 815 °C tests in figures 12 and 13. Both test methods at 425 °C resulted in approximately the same amount of inelastic strain (0.10 percent) after the first cycle as did both test methods at 815 °C, which exhibited 0.04 percent inelastic strain after the first cycle. For both test methods at both temperatures, the hysteresis did not close (i.e., did not become a loop) upon the first reverse cycle since neither control program allowed the composite to experience compressive stress. However, in all subsequent cycles, complete hysteresis loops were evident. For the 425 °C strain-controlled test, the inelastic strain decreased to zero before the first abrupt stress drop and increased again thereafter. The 425 °C load-controlled test and the 815 °C strain-and load-controlled tests all exhibited approximately constant inelastic strain (measured from hysteresis widths) from the second through final cycles at 0.005, 0.02, and 0.04 percent, respectively. Both the 425 and 815 °C strain-controlled tests exhibited modulus degradation simultaneously with the abrupt stress decreases as previously discussed in figures 8 and 9. In contrast, the load-controlled tests at 425 and 815 °C exhibited approximately constant modulii throughout the tests with no stiffness degradation before failure. In this discussion of fatigue response, it is important to note that the usual meaning of inelastic strain and hysteresis for monolithic materials may be different than its definition for composites. Inelastic deformation for composites may be due to one or more of events such as matrix deformation, matrix cracking, fiber/matrix debonding, or fiber fracture. It is not possible to attribute particular types of damage to inelastic behavior until metallographic work is completed. However, the abrupt decreases in strength and modulus in the strain-controlled tests can certainly be presumed to have involved at least fiber fracture in order to have obtained such large quantities of degradation. This reasoning relies on the facts that the fibers provide the majority of the strength and stiffness in this composite (ref. 9) and that the decreases in strength and stiffness occurred simultaneously as would be expected with fiber fracture.

Two other general observations can be made from the stress-strain responses of figures 10 to 13 which result from the type of test method used. In the strain-controlled tests of figures 10 and 12, the maximum stress of the composite decreased slowly in the cycles before the first abrupt stress drop. These stress decreases could be attributed to one or more of the following: softening, fatigue damage, or effects of the test control program. Since the test control program did not allow compressive stresses to be induced, the strain-controlled specimens actually experienced smaller strain amplitudes with each cycle, as can be seen in figures 10 and 12 and by examining the continuously increasing minimum strain in figure 9. Thus, it was possible that the test control mode was influential in continuously reducing the stress at the maximum control strain as it induced the continuously smaller strain amplitudes throughout the test. The possible contributions of material softening and decreased stress due to control mode could not be determined from these tests; increasing the strain amplitude after particular cycles would be necessary to characterize this behavior. In the load-controlled tests, strain ratchetting was observed up to 0.08 percent at 425 °C, which was 18 percent of the total strain, and up to 0.12 percent, which was 25 percent of the total strain, was observed at 815 °C. For both Regions I and II, strain ratchetting at 425 °C was less than at 815 °C, presumably due to the difference in creep rate of the matrix at the two temperatures (ref. 18).

Region III of figure 3 incorporates the high cycle fatigue lives of the SiC/Ti-24Al-11Nb composite with lives $\geq 10^5$ cycles. The maximum stresses and strains were so low in this regime that the specimens were typically run-outs. No indications of damage, such as stress drops for the strain-controlled sample, were observed. Therefore, tests were discontinued after 10^5 cycles. The strain- and load-controlled samples at 425 °C and the strain-controlled sample at 815 °C appeared to establish an endurance limit at approximately 0.3 percent strain for this SiC/Ti-24Al-11Nb composite.

As previously mentioned, Talreja's (ref. 1) concept of the fatigue life diagram, figure 4, was developed for polymer matrix composites at 23 °C. Three distinct regions were evident, each with a different dominant fatigue mechanism. For polymer matrix composites, Region I represented the region where fiber fracture and interfacial debonding were the dominant mechanisms of damage. This region's width represented the scatter in the monotonic fracture strain of the composite. The scatter in this band depicted the fiber's probabilistic failure nature and was associated with low cycle fatigue lives. In Region II, matrix cracking and interfacial shear failure were the dominant mechanisms. Region III began at the fatigue limit of the matrix and the dominant damage mechanism for polymer matrix composites in this region was matrix microcrack nucleation. This region was associated with high cycle fatigue lives and usually resulted in test runouts.

While the fatigue lives of the SiC/Ti-24Al-11Nb composite at 425 and 815 °C showed similar shapes in the three regions as compared to the polymer matrix composites, much of the damage mechanisms for the isothermally fatigued SiC/Ti-24Al-11Nb composite remains to be determined. Fatigue tests of the Ti-24Al-11Nb matrix are also necessary to estimate the contribution of matrix inelastic deformation in the composite in each of the three regions. Matrix tests are also necessary to determine whether Region III began at the fatigue limit of the matrix. However, as discussed previously, differences in fatigue response and fatigue failure imply certain mechanisms within each region. It appeared that Region I was dominated by catastrophic fiber fracture, particularly at low numbers of cycles-to-failure, though other mechanisms may also have been operative. In Region II, it appeared likely that the abrupt stress decreases observed in strain-control were associated, at least in part, by local fiber fracture(s) since these stress decreases were accompanied by large modulus decreases. In Region III, fatigue life of the SiC/Ti-24Al-11Nb composite was similar to polymer matrix composites (ref. 1) in that only test runouts were observed in this region.

TEST CONTROL MODE

Since the development of the Manson-Coffin (refs. 19 and 20) relationship, strain-controlled tests have been prevalent in the fatigue testing of monolithic, polycrystalline materials. Mitchell (ref. 21) has presented several fundamental reasons for preferring strain-control over load-control. Two of the most important were that strain-control provides a kinematic constraint which does not allow ratchetting to take place and that strain-control provides a scenario most often like an actual component; i.e., stress-strain gradients exist in many practical applications causing material at critical locations to be constrained to some extent.

Recent studies investigating high temperature fatigue of metal matrix continuous fiber composites (refs. 22 to 24) used load-control for other practical reasons. Chief among them was the fact that the materials were available only in the form of thin plates. Thus, there was the very real possibility of producing significant compressive stresses and buckling of the composite specimens due to geometric restraints if tested in strain-control. By conducting these tests in load-control, specimen buckling was alleviated but in exchange, ratchetting was produced. In the present study, load-controlled testing also produced ratchetting of up to 19 percent of the total strain range at 815 °C in Region II.

In addition to the present study, one previous study on SiC/Ti-24Al-11Nb has used strain-control without specimen buckling (ref. 12). In the present study, cyclic tests were conducted with computer control in a manner which was strain controlled and load monitored. In these tests, the specimen was loaded to a maximum strain and then unloaded to zero stress. This method did not allow the specimen to experience compressive stresses and by design, did not allow ratchetting to occur. However, as previously discussed and as shown in figures 10 and 12 for SiC/Ti-24Al-11Nb, the control program imposed successively smaller strain amplitudes on the composite as it controlled to zero stress on the reverse cycle. Thus, the tension-tension strain-control mode provided less and less severity as the test progressed. However, it is believed that this type of test is justified since thin plates of continuous fiber composite are not suitable for applications involving fully reversed cycling with compressive loads in the fiber direction.

In addition to the successively smaller strain ranges and the ratchetting discussed above, the type of test control mode (tension-tension strain-control versus tension-tension load-control) used in the fatigue of this SiC/Ti-24Al-11Nb composite was seen to produce other instances of different material response. The most striking differences in behavior occurred in Region II and will be summarized here along with the similarities.

The primary similarity in the fatigue response of the SiC/Ti-24Al-11Nb composite in strain- and load-controlled testing occurred on the first cycle, where both types of tests produced a large quantity of inelastic strain. This inelastic strain was equal in both types of tests at equivalent strain amplitude and at a given temperature. Also, the inelastic strain of the first cycle was greater than that produced on any subsequent cycle in both types of tests. Therefore, metallographic examination of interrupted tests from either test control mode would be expected to result in the determination of equivalent mechanisms after the first cycle of either test. Furthermore, if one were primarily concerned with determining life of the composite, either strain- or load-controlled testing would generate this information, provided an appropriate definition for failure in strain-controlled tests is used.

The primary differences between test control modes obtained with SiC/Ti-24Al-11Nb occurred late in the test, at the first abrupt stress drop and beyond. Complete fracture in the load-controlled tests occurred catastrophically and coincided with the first abrupt stress drop observed in the strain-controlled tests, as shown in figure 8. Thus, an advantage of strain-controlled testing is that it allows easier identification of the failure mechanism by interruption and examination of a specimen after the stress drop has occurred. The other difference in test control mode involved the definition of fatigue life in strain-control. Even after the first abrupt stress drop, defined as failure in this study, the composite continued to have appreciable load-carrying capacity for many thousands of cycles. If an application were most similar to the tension-tension strain-controlled tests, the SiC/Ti-24Al-11Nb composite may be considered to have a longer useful life than that indicated by the load-controlled tests.

CONCLUSIONS

1. A fatigue life diagram was beneficial in identifying three distinct regions of behavior in the SiC/Ti-24Al-11Nb composite. Regions I and III did not vary with test temperature and Region II was temperature dependent. Furthermore, distinct damage mechanisms are also expected to be defined in these regions.

2. SiC/Ti-24Al-11Nb fatigue failure within Region I was defined as catastrophic and appeared to be fiber dominated although other mechanisms may be operative. Fatigue behavior in Region II was defined as progressive since the strain-controlled tests exhibited first gradual decreases in stress and then abrupt, simultaneous decreases in strength and modulus during the life of the composite. In the high cycle fatigue regime of Region III, an apparent endurance limit at 0.3 percent strain was observed.

3. The definition of failure used for the strain-controlled tests in Region II (the first abrupt, simultaneous decrease in strength and modulus) was a suitable approach since it produced fatigue lives in close agreement with lives from load-controlled tests which were determined by complete fracture.

4. The advantages of using the tension-tension strain-controlled test method were that specimen buckling was prevented while still providing a strain-control type of test and stable fatigue cycling continued after large, abrupt decreases in load-carrying capacity. This allows easy interruption and inspection of fatigue damage. The disadvantage of this test method was the application of a continuously decreasing strain amplitude caused a continuous decrease in the severity of the test.

5. The advantage of using load-controlled testing was that failure was unambiguously defined. The disadvantages were that ratchetting was induced and stable fatigue cycling was not possible after a large reduction in the composite's load-carrying capability.

6. Since each type of test control mode has unique features and results in unique fatigue response both strain- and load-controlled tests are important to the complete understanding of SiC/Ti-24Al-11Nb composite fatigue behavior.

ACKNOWLEDGEMENT

The authors gratefully acknowledge the diligence and expertise of R.M. Shinn of Sverdrup Technology, Inc. in the Fatigue Laboratory.

REFERENCES

1. Talreja, R., Fatigue of Composite Materials, Technomic Publishing Co., Lancaster, PA, 1987.

2. Brindley, P.K., in High-Temperature Ordered Intermetallic Alloys II; Proceedings of the Second Symposium, Boston, MA, Dec. 1986, N.S. Stoloff, C.C. Koch, C.T. Liu, and Izumi, Eds., (MRS Symposia Proceedings, Vol. 81), Materials Research Society, Pittsburgh, PA, 1987, pp. 419-424.

3. Brindley, P.K., Bartolotta, P.A., and Klima, S.J., "Investigation of a SiC/Ti-24Al-11Nb Composite," NASA Report TM-100956, National Aeronautics and Space Administration, Lewis Research Center, Cleveland, OH, 1988.

4. Baumann, S.F., Brindley, P.K., and Smith, S.D., "Reaction Zone Microstructure in a Ti_3Al+Nb/SiC Composite," Presented at the 1988 TMS Fall Meeting, Sept. 26-29, Chicago, IL. To be published.

5. Bowden, D.M.; Sastry, S.M.L.; and Smith, P.R., Scripta Metallurgica, Vol. 23, No. 3, Mar. 1989, pp. 407-410.

6. Rhodes, C.G., Amato, R.A., and Spurling, R.A., "Fiber-Matrix Interactions in SiC Reinforced Titanium Aluminides," Presented at the Symposium on High Temperature Composites, American Society for Composites, Dayton, OH, June 1989.

7. Yang, C.J., Jeng, S.M., and Yang, J.-M., Scripta Metallurgica, Vol. 24, No. 3, March 1990, pp. 469-474.

8. Eldridge, J.I, and Brindley, P.K., Journal of Materials Science Letters, Vol. 8, No. 12, Dec. 1989, pp. 1451-1454.

9. Brindley, P.K., Draper, S.L., Nathal, M.V., and Eldridge, J.I., in Fundamental Relationships Between Microstructures and Mechanical Properties of Metal Matrix Composites, P.K. Liaw and M.N. Gungor, Eds., TMS, Pittsburgh, PA, 1989, pp. 387-401.

10. Russ, S.M., "Thermal Fatigue of Ti-24Al-11Nb/SCS-6," Presented at the 1988 TMS Fall Meeting, Sept. 26-29, Chicago, IL. To be published.

11. Brindley, P.K., Bartolotta, P.A., and MacKay, R.A., "Thermal and Mechanical Fatigue of SiC/Ti_3Al+Nb," in HiTemp Review 1989: Advanced High Temperature Engine Materials Technology Program, NASA Report CP-10039, National Aeronautics and Space Administration Lewis Research Center, Cleveland, OH., 1989.

12. Bain, K.R., and Gambone, M.L., "Fatigue and Fracture of Titanium Aluminides," Vols. I and II. WRDC-TR-89-4145, 1989.

13. Pickens, J.W., Noebe, R.D., Watson, G.K., Brindley, P.K., and Draper, S.L., "Fabrication of Intermetallic Matrix Composites by the Powder Cloth Process," NASA Report TM-102060, National Aeronautics and Space Administration, Lewis Research Center, Cleveland, OH, 1989.

14. Bartolotta, P.A., and McGaw, M.A., "A High Temperature Fatigue and Structures Testing Facility," NASA Report TM-100151, National Aeronautics and Space Administration, Lewis Research Center, Cleveland, OH, 1987.

15. Brindley, P.K., "Furnace for Tensile/Fatigue Testing," U.S. Patent Application Serial No. 382885.

16. Kelly, A., and Davies, G.J., Metallurgical Reviews, Vol. 10, No. 37, 1965, pp. 1-77.

17. Salkind, M.J., in Composite Materials: Testing and Design; Proceedings of the Second Conference, (also ASTM STP-497, 1972) ASTM, Philadelphia, PA, 1972, pp. 143-169.

18. Hayes, R.W., Scripta Metallurgica, Vol. 23, No. 11, Nov. 1989, pp. 1931-1936.

19. Manson, S.S., "Behavior of Materials Under Conditions of Thermal Stress," NACA Report TN-2933, National Advisory Committee for Aeronautics, 1953.

20. Coffin, L.F., Jr., ASME Transactions, Vol. 76, 1954, pp. 931-950.

21. Mitchell, M.R., in Fatigue and Microstructure, ASM Materials Science Seminar, ASM, St. Louis, MO, 1978, pp. 385-437.

22. Verrilli, M.J., Kim, Y.S., and Gabb, T.P., "High Temperature Fatigue Behavior of Tungsten Copper Composites," NASA Report TM-102404, National Aeronautics and Space Administration, Lewis Research Center, Cleveland, OH, 1989.

23. Castelli, M.G., Bartolotta, P.A., Ellis, R., Ervin, D.R., and Heine, T.E., "Development of Thermomechanical Testing Techniques for Advanced Composite Materials," in High Temp Review 1989: Advanced High Temperature Engine Materials Technology Program, NASA Report CP-10039, National Aeronautics and Space Administration, Lewis Research Center, Cleveland, OH, 1989.

24. Gayda, J., Gabb, T.P., and Freed, A.D., "The Isothermal Fatigue Behavior of a Unidirectional SiC/Ti Composite and the Ti Alloy Matrix," NASA Report TM-101984, National Aeronautics and Space Administration, Lewis Research Center, Cleveland, OH, 1989.

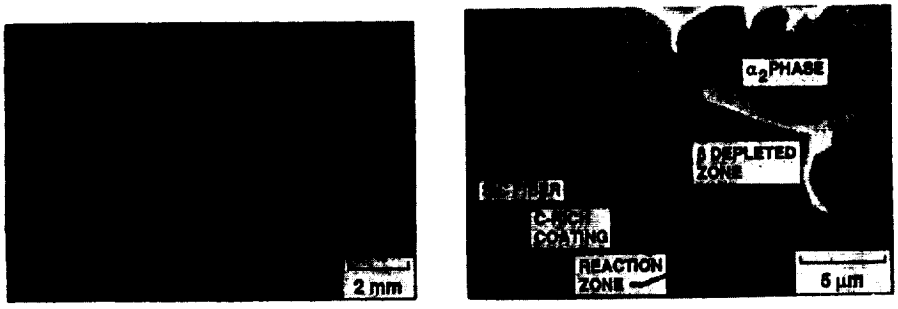

(a) Typical fiber distribution. (b) Microstructure near fiber-matrix interface.

Figure 1. - As-fabricated SiC/Ti-24Al-11Nb composite.

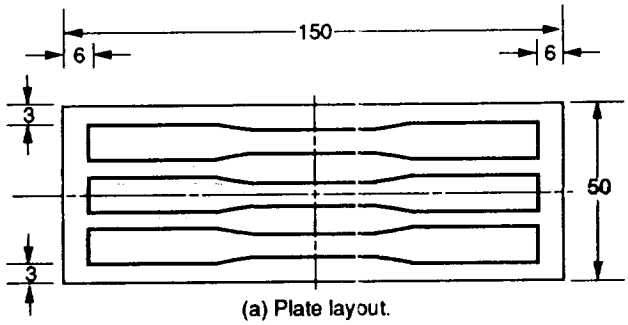

(a) Plate layout.

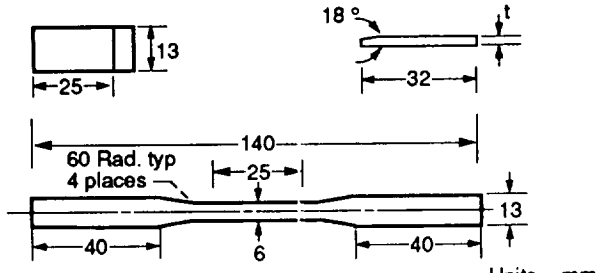

(b) Geometry and tab details. Units = mm

Figure 2. - Test specimen details.

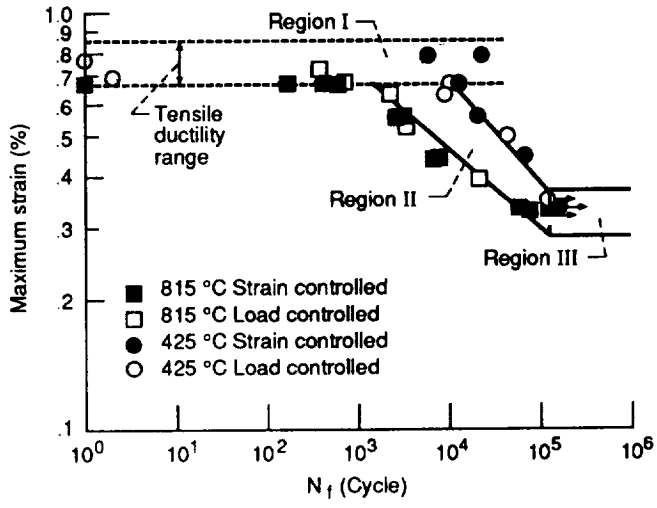

Figure 3. - Fatigue life diagram of SiC/Ti-24Al-11Nb at elevated temperatures.

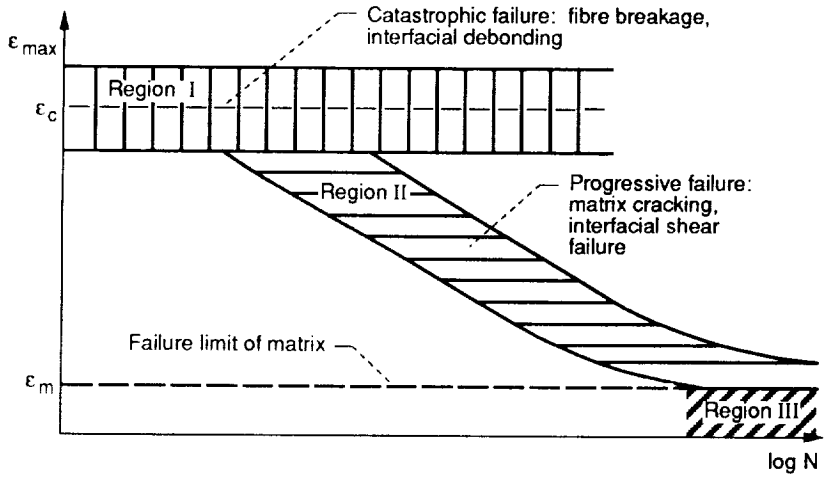

Figure 4. - Talreja's fatigue life diagram for unidirectional polymer matrix composites at room temperature.

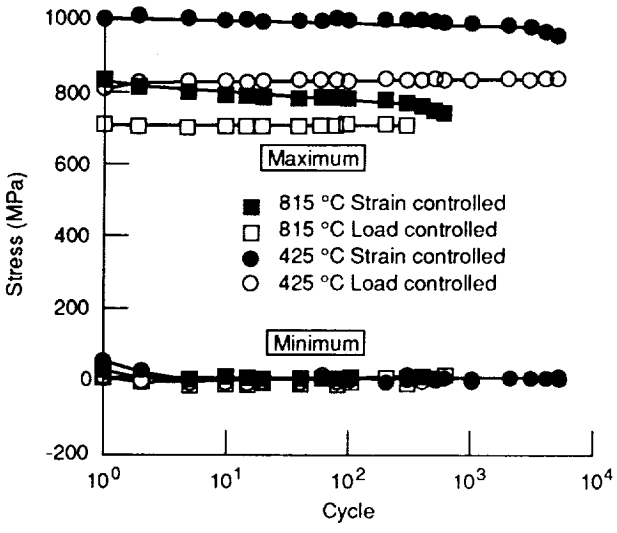

Figure 5. - Variation of maximum and minimum stress for region I tests.

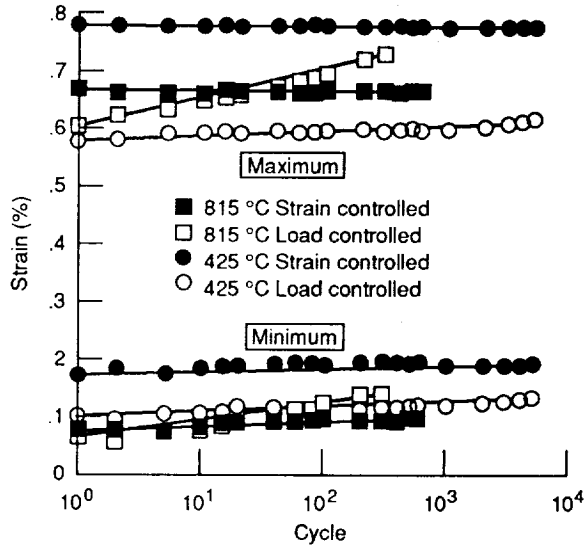

Figure 6. - Variation of maximum and minimum strain for region I tests.

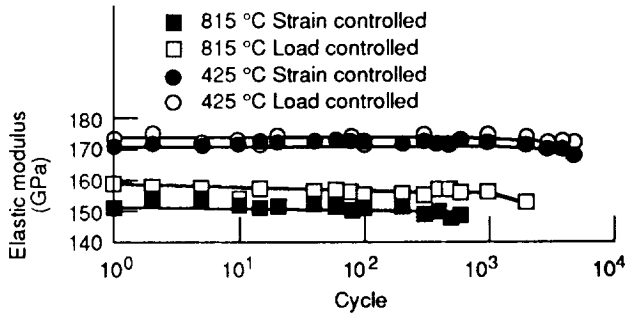

Figure 7. - Variation of elastic modulus for region I tests.

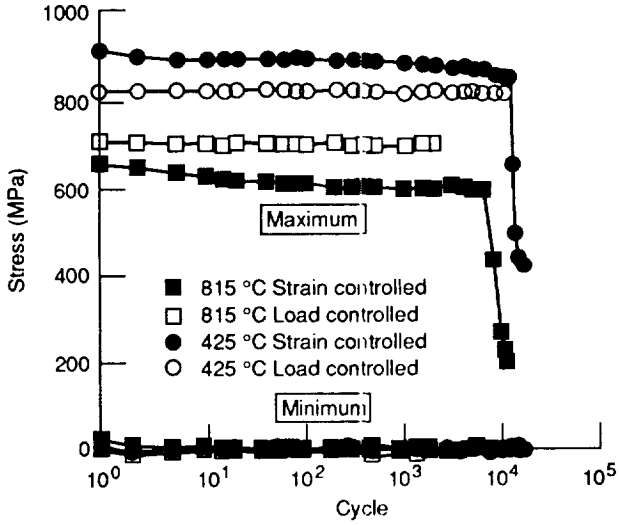

Figure 8. - Variation of maximum and minimum stress for region II tests.

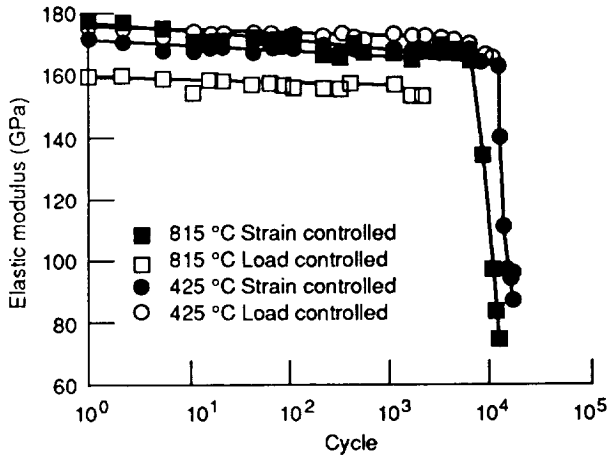

Figure 9. - Variation of elastic modulus for region II tests.

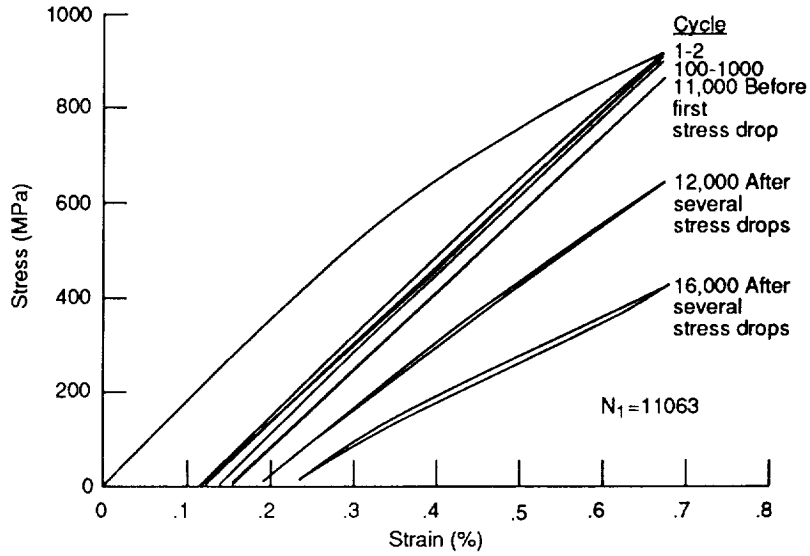

Figure 10. - Typical stress-strain response of SiC/Ti-24Al-11Nb conducted at 425 °C with ε_{max} = 0.67% under strain control (region II).

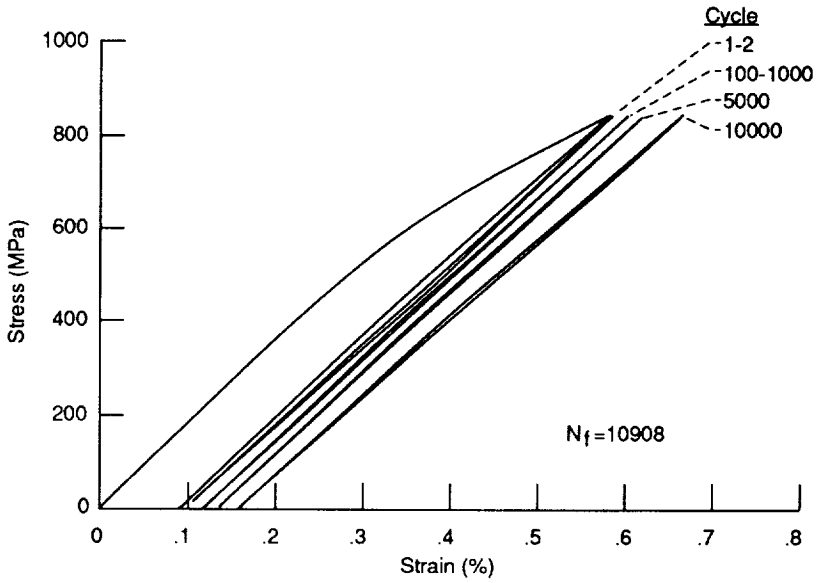

Figure 11. - Typical stress-strain repsponse of SiC/Ti-24Al-11Nb conducted at 425 °C with σ_{max} = 830 MPa under load control (region II).

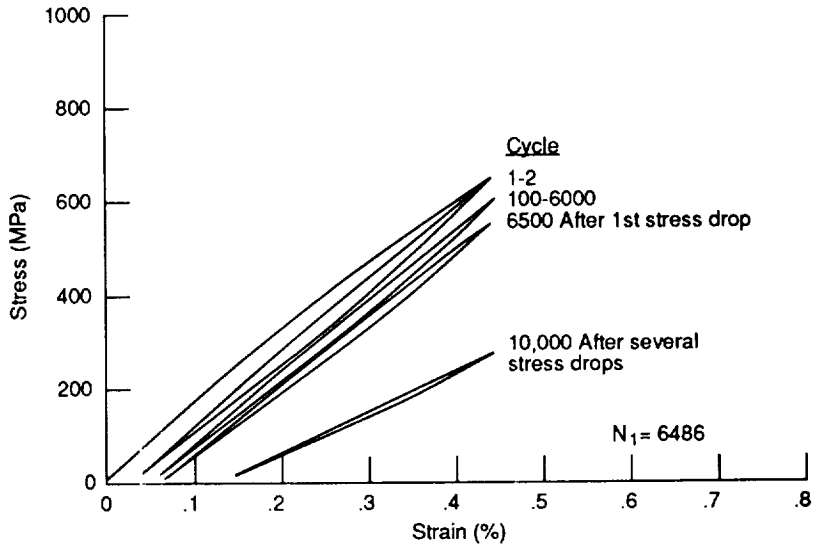

Figure 12. - Typical stress-strain response of SiC/Ti-24Al-11Nb conducted at 815 °C with ε_{max} = 0.45% under strain control (region II).

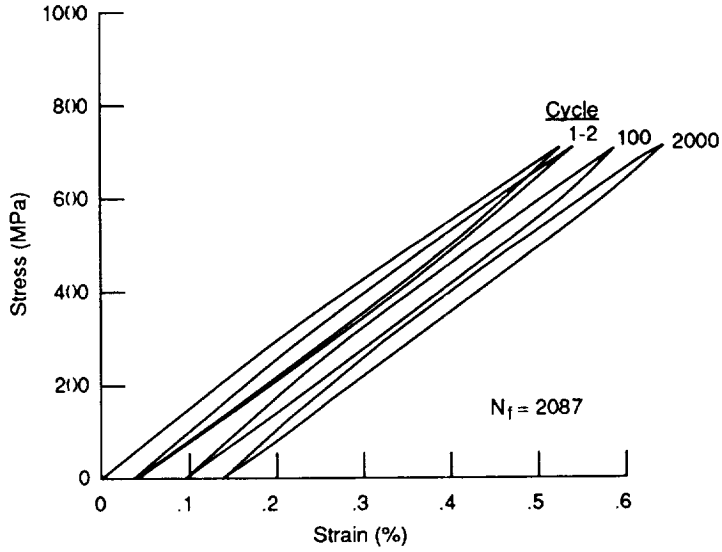

Figure 13. - Typical stress-strain response of SiC/Ti-24Al-11Nb conducted at 815 °C with σ_{max} = 710 MPa under load control (region II).

NASA
National Aeronautics and Space Administration

Report Documentation Page

1. Report No.	2. Government Accession No.	3. Recipient's Catalog No.
NASA TM-103157		

4. Title and Subtitle	5. Report Date
High Temperature Fatigue Behavior of a SiC/Ti-24Al-11Nb Composite	6. Performing Organization Code

7. Author(s)	8. Performing Organization Report No.
P.A. Bartolotta and P.K. Brindley	E-5524
	10. Work Unit No. 510-01-0A

9. Performing Organization Name and Address	11. Contract or Grant No.
National Aeronautics and Space Administration Lewis Research Center Cleveland, Ohio 44135-3191	13. Type of Report and Period Covered Technical Memorandum

12. Sponsoring Agency Name and Address	14. Sponsoring Agency Code
National Aeronautics and Space Administration Washington, D.C. 20546-0001	

15. Supplementary Notes

Prepared for the 10th Symposium on Composite Materials: Testing and Design sponsored by the American Society for Testing Materials, San Francisco, California, April 24-25, 1990.

16. Abstract

A series of tension-tension strain- and load-controlled fatigue tests were conducted on unidirectional SiC/Ti-24Al-11Nb (at %) composites at 425 and 815 °C. Several regimes of damage were identified using Talrega's (ref. 1) concept of fatigue life diagrams. Issues of test technique, test control mode, and definition of failure were also addressed.

17. Key Words (Suggested by Author(s))	18. Distribution Statement
Fatigue; Composites; Titanium aluminide; Silicon carbide; Test methods	Unclassified – Unlimited Subject Category 39

19. Security Classif. (of this report)	20. Security Classif. (of this page)	21. No. of pages	22. Price*
Unclassified	Unclassified	14	A03

NASA FORM 1626 OCT 86

*For sale by the National Technical Information Service, Springfield, Virginia 22161